JVI Journals.ASM.org

The ATR Signaling Pathway Is Disabled during Infection with the Parvovirus Minute Virus of Mice

Richard O. Adeyemi,* David J. Pintel

Department of Molecular Microbiology and Immunology University of Missouri—Columbia, School of Medicine, Bond Life Sciences Center, Columbia, Missouri, USA

ABSTRACT

The ATR kinase has essential functions in maintenance of genome integrity in response to replication stress. ATR is recruited to RPA-coated single-stranded DNA at DNA damage sites via its interacting partner, ATRIP, which binds to the large subunit of RPA. ATR activation typically leads to activation of the Chk1 kinase among other substrates. We show here that, together with a number of other DNA repair proteins, both ATR and its associated protein, ATRIP, were recruited to viral nuclear replication compartments (autonomous parvovirus-associated replication [APAR] bodies) during replication of the single-stranded parvovirus minute virus of mice (MVM). Chk1, however, was not activated during MVM infection even though viral genomes bearing bound RPA, normally a potent trigger of ATR activation, accumulate in APAR bodies. Failure to activate Chk1 in response to MVM infection was likely due to our observation that Rad9 failed to associate with chromatin at MVM APAR bodies. Additionally, early in infection, prior to the onset of the virus-induced DNA damage response (DDR), stalling of the replication of MVM genomes with hydroxyurea (HU) resulted in Chk1 phosphorylation in a virus dose-dependent manner. However, upon establishment of full viral replication, MVM infection prevented activation of Chk1 in response to HU and various other drug treatments. Finally, ATR phosphorylation became undetectable upon MVM infection, and although virus infection induced RPA32 phosphorylation on serine 33, an ATR-associated phosphorylation site, this phosphorylation event could not be prevented by ATR depletion or inhibition. Together our results suggest that MVM infection disables the ATR signaling pathway.

IMPORTANCE

Upon infection, the parvovirus MVM activates a cellular DNA damage response that governs virus-induced cell cycle arrest and is required for efficient virus replication. ATM and ATR are major cellular kinases that coordinate the DNA damage response to diverse DNA damage stimuli. Although a significant amount has been discovered about ATM activation during parvovirus infection, involvement of the ATR pathway has been less studied. During MVM infection, Chk1, a major downstream target of ATR, is not detectably phosphorylated even though viral genomes bearing the bound cellular single-strand binding protein RPA, normally a potent trigger of ATR activation, accumulate in viral replication centers. ATR phosphorylation also became undetectable. In addition, upon establishment of full viral replication, MVM infection prevented activation of Chk1 in response to hydroxyurea and various other drug treatments. Our results suggest that MVM infection disables this important cellular signaling pathway.

In response to DNA damage stimuli and infection by DNA viruses, cells mount a complex signaling cascade called the DNA damage response (DDR) that results in alterations in a myriad of cellular activities, including cell cycle progression, DNA repair, and in some cases apoptosis (1, 2). The DDR is orchestrated by a series of posttranscriptional modifications, including phosphorylation, ubiquitination, and sumoylation, which lead to accumulation of checkpoint, DNA repair, and other effector proteins at the vicinity of the DNA lesion (3, 4). At the core of this response are a number of well-conserved phosphatidylinositol 3-kinase-related kinases (PIKKs) which coordinate the DDR following their rapid redistribution to the site of the DNA lesion. Once there, they phosphorylate a number of cellular targets, including local chromatin components (5). The three major PIKKs which control DDR signaling are ataxia telangiectasia mutated (ATM), ataxia telangiectasia and Rad-3 related (ATR), and DNA-dependent protein kinase (DNA PK) (6–8).

ATM and DNA PK predominantly respond to deleterious double-strand breaks (DSBs) which can arise following ionizing radiation treatment (9). Unlike the other two kinases, ATR is essential for cellular survival, and it responds to various DNA lesions associated with cellular replication in S and G_2 phases (10, 11). The exact process by which ATR is activated is complex and incompletely understood. ATR is recruited to RPA-coated single-stranded DNA (ssDNA) at DNA damage sites via its interacting partner, ATRIP, which binds to the large subunit of RPA (12). In a separate recruitment event, the chromatin protein Rad17 loads the heterotrimeric ring-shaped 9-1-1 complex (which consists of Rad9, Hus1, and Rad1 and resembles the replication sliding clamp, PCNA) onto free 5′ ends at stalled replication forks and recessed DNA ends (13–15). Full activation of ATR requires TOPBP1, which is recruited to DNA lesions via the 9-1-1 complex (16, 17), although recent reports indicate that the Mre11,

Received 15 May 2014 **Accepted** 18 June 2014

Published ahead of print 25 June 2014

Editor: M. J. Imperiale

Address correspondence to David J. Pintel, pinteld@missouri.edu.

* Present address: Richard O. Adeyemi, Department of Genetics, Harvard Medical School, Boston, Massachusetts, USA.

doi:10.1128/JVI.01412-14

Rad50,and Nbs1 (MRN) complex might also be involved in recruitment of TOPBP1 (18, 19). The Rad17/9-1-1 complex also interacts with claspin, a Chk1 binding partner that recruits Chk1 to ATR and is essential for Chk1 phosphorylation (20–23). Phosphorylation of Chk1 by activated ATR results in a number of cellular effects, including, among others, checkpoint activation in S and G_2 phases, inhibition of new replication origin firing, and stabilization of replication forks (24, 25). Thus, ATR activities are mediated in large part by Chk1, and as a result, the phosphorylation status of Chk1 has been employed as a surrogate for ATR activation.

We and others have previously reported that parvoviruses activate an ATM-dependent DNA damage signaling cascade characterized by phosphorylation of H2AX, Nbs1, Chk2, p53, and other DDR-related proteins (26–32). This response governs the virus-induced cell cycle arrest and is required for efficient parvovirus replication (26, 33–36). Parvoviral genomes have unique single-stranded DNA structures with hairpins at both ends. The parvovirus minute virus of mice (MVM) forms compartments within the nucleus called autonomous parvovirus-associated replication (APAR) bodies (37, 38), which are sites for ongoing viral replication, during which large amounts of replication intermediates with unusual DNA structures are produced. Not surprisingly, these sites are enriched for a number of DNA repair proteins. In addition, there is marked redistribution of the cellular RPA protein to these bodies, which would be predicted to recruit and activate ATR; however, caffeine (which inhibits both ATM and ATR) did not inhibit MVM replication significantly more than an ATM inhibitor alone, and Chk1 was not activated (26).

Our results suggested that a detailed investigation of how ATR signaling was affected during parvovirus infection was warranted. Although MVM infection induces an S/G2 cell cycle block required for successful infection, p21 and Chk1, major effectors typically associated with S-phase and G_2-phase cell cycle arrest in response to diverse DNA damage stimuli, are either depleted or inactive, respectively, during MVM infection (26, 27, 39). We have recently shown, however, that the MVM-induced DDR resulted in significant depletion of cyclin B1, thus directly inhibiting cyclin B1-CDK1 complex function and preventing mitotic entry (33). In this work, we have investigated the regulation of the ATR signaling pathway following MVM infection. We have shown that ATR and ATRIP were recruited to viral replication compartments, yet ATR signaling to Chk1 was disabled. Upon full viral infection and replication, MVM also prevented Chk1 phosphorylation in response to treatment with exogenous DNA-damaging agents that normally result in its activation. Failure to activate Chk1 during viral infection was not due to degradation of specific components of the ATR signaling pathway; rather, the Rad9 protein, which as part of the 9-1-1 complex is required for Chk1 activation, was found not to be associated with chromatin during infection.

MATERIALS AND METHODS

Cells, viruses, and infections. All experiments were performed interchangeably in murine A9 cells and human 324K cells, which were propagated as previously described (26). The wild-type fibrotropic MVMp strain was used for all infections. Infections were performed at a multiplicity of infection (MOI) of 10 unless otherwise indicated. UV inactivation of wild-type MVMp was carried out as previously described (26).

Cell synchronization and drug treatments. Where indicated, A9 cells were parasynchronized using isoleucine-deprived medium as previously described (39). The experiment shown in Fig. 2C was performed using a previously described double block procedure (40). Aphidicolin treatment was performed for 16 h at 12 μg/ml. Hydroxyurea was obtained from Calbiochem and used at the indicated concentration. Neocarzinostatin was obtained from Sigma and used at 150 ng/ml.

Antibodies. Commercially available antibodies used in this study were from Cell Signaling (Chk1, catalog 2345S; Chk1-P-S345, catalog number 2348S; and ATR, catalog number 2790S), GeneTex (RPA32, catalog number GTX70258; Hus1, catalog number GTX62975), Bethyl (TOPBP1, catalog number A300-111A; RPA32-P-S4/8, catalog number A300-245A; and RPA-P-S33, catalog number A300-246A), Millipore (ATRIP, catalog number 07-625; histone H3, catalog number 05-928; γH2AX, catalog number 05-636), Santa Cruz Biotechnology (Claspin, catalog number sc-376773; Rad17, catalog number sc-5613; Rad9, catalog number sc-8324; Rad1, catalog number sc-22783; and ATR, catalog number sc-1887), and Kerafast (ATR-P-T1989, catalog number EVU001). Secondary antibodies for immunofluorescence (IF) and Western blotting and antibodies against NS1, actin, and tubulin have been previously described (26).

siRNA transfections. ON-TARGETplus Smart pool small interfering RNAs (siRNAs) directed against human and mouse ATR were obtained from Dharmacon. Negative-control siRNAs were obtained from Qiagen. Cells were transfected using the HiPerfect reagent (Invitrogen) as previously described (33).

Immunoblot analyses. Cells grown and infected in 60-mm dishes were harvested and lysed in radioimmunoprecipitation assay (RIPA) buffer containing protease and phosphatase inhibitors. The protein concentration was determined by Bradford assay. For the experiment shown in Fig. 2A, whole-cell lysates were prepared by lysing cells directly in 2% SDS lysis buffer. Western blot analyses were performed as previously described (26).

Cell fractionation and ATR phosphorylation assay. Cell fractionation experiments were performed using previously described cell fractionation protocols and assessed by monitoring the presence or absence of chromatin-associated histone H3 (41, 42). The chromatin pellet (P3 fraction) was resuspended in 2% SDS lysis buffer and processed for Western blot analyses. Determination of ATR phosphorylation status was modified from a previously described protocol (43). Briefly, after fractionation of harvested cells as described above, the chromatin pellet (P3 fraction) was resuspended in Tris lysis buffer (containing 10 mM Tris [pH 8.0], 150 mM NaCl, 10 mM EDTA, and 1% NP-40) with 2% SDS. Samples were boiled and then diluted with Tris lysis buffer without SDS to a final SDS concentration of 0.2%. Lysates were immunoprecipitated using 4 μg of ATR antibody overnight at 4°C and pulled down with protein G beads. After extensive washing, beads were resuspended in protein loading buffer and processed for Western blot analyses.

Immunofluorescence analyses. Assays were performed as previously described (39). Briefly, cells were grown on coverslips in 6-well plates, washed, preextracted in CSK buffer (39) to remove soluble, non-chromatin-associated proteins, and then fixed in 4% paraformaldehyde. Antibodies were diluted in 3% bovine serum albumin (BSA) in phosphate-buffered saline (PBS). Nuclei were visualized by staining with 4′,6-diamidino-2-phenylindole (DAPI). Coverslips were mounted in Floromount-G (Southern biotech), and images were obtained using a Zeiss LSM 5 live confocal microscope. All images were captured using a 63× objective.

RESULTS

Viral replication is insufficient for Chk1 activation during MVM infection. We previously reported that MVM infection results in ATM-mediated phosphorylation of a number of DDR-related proteins, including p53 and the checkpoint kinase Chk2 (26). As discussed, replication of the single-stranded MVM ge-

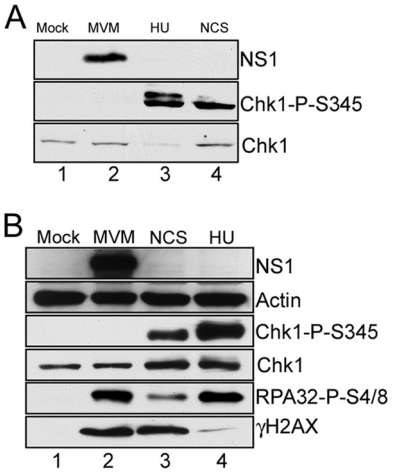

FIG 1 Viral replication is insufficient for Chk1 activation during MVM infection. (A) Murine A9 cells were infected with MVM at an MOI of 10 for 24 h. Uninfected control cells were treated with 1 mM hydroxyurea (HU) for 12 h or 150 ng/ml of neocarzinostatin (NCS) for 1 h. Cells were harvested and processed for Western blotting using antibodies directed against the indicated proteins. (B) Human 324K cell lines were treated as mentioned above for A9 cells. Cells were harvested, and RIPA lysates were blotted using antibodies directed against the indicated proteins.

nome, which proceeds through the displacement of single-stranded MVM DNA presumably coated with cellular RPA, would be predicted to recruit ATR and potentially activate its downstream target Chk1. However, our previous results did not identify a role for ATR activation in MVM replication, nor did we detect Chk1 phosphorylation following MVM infection (26). This suggested that ATR was not fully activated, which has also been suggested by others (31).

Figure 1A demonstrates that whereas treatment of cells with hydroxyurea, which inhibits ribonucleotide reductase, leading to stalling of replication forks (44), induced Chk1 phosphorylation in murine A9 cells (Fig. 1A, lane 3), MVM infection did not (Fig. 1A, lane 2). Lack of Chk1 phosphorylation by MVM was not due to depletion of total Chk1 (Fig. 1A, compare lanes 1 and 2). In these experiments, treatment with hydroxyurea (HU) resulted in a reduction in Chk1 protein levels, consistent with previous reports of targeted Chk1 degradation following its activation (45–47) (Fig. 1A, lane 3). ATM is activated mainly by double-stranded breaks (48, 49). Double-strand breaks in S phase are resected by the CTIP-MRN complex to generate single-stranded DNA, which in turn leads to ATR activation and homologous recombination-mediated repair (50–52). Thus, there is typically an ATM-ATR switch that occurs in response to DSBs (53), and consequently, treatment with agents that activate ATM can also lead to Chk1 phosphorylation in the S/G2 population (54, 55). Since MVM activates ATM without detectable Chk1 phosphorylation, we tested whether resection activity occurred normally in these cells. Treatment with neocarzinostatin (NCS), a radiomimetic drug which, like MVM, induces a DDR mediated primarily by ATM (56, 57), also resulted in robust Chk1 phosphorylation (Fig. 1A, lane 4), as has been reported for other cell types (58), suggesting that failure to observe Chk1 phosphorylation during MVM infection was not due to blockage of an ATR-activating resection activity in these cells.

The failure to activate Chk1 was also seen following infection of permissive human 324K cells. Similarly to the case with murine A9 cells, treatment of 324Ks with both NCS (Fig. 1B, lane 3) and HU (Fig. 1B, lane 4) resulted in significant phosphorylation of Chk1; however, MVM infection did not do so (Fig. 1B, lane 2). Importantly, as previously observed (26), under the conditions tested, other aspects of the DNA damage response were potently activated in MVM-infected 324K cells and were comparable to or higher than those seen following drug treatment. For example, MVM infection resulted in significant ATM-dependent (26) phosphorylation of H2AX, similar to that seen following NCS treatment (Fig. 1B, compare lanes 2 and 3) and substantially higher than that in response to HU treatment, which causes DSBs only upon fork collapse (Fig. 1A, compare lanes 2 and 4). In addition, there was robust ATM and DNA PK-dependent (26) phosphorylation of RPA on S4/8 that was similar to that seen following HU treatment and considerably higher than that following treatment with NCS (Fig. 1B, compare lane 2 to lanes 3 and 4). NCS activation of RPA32 was likely lower because NCS induces RPA phosphorylation only in the resected S/G2 phase population. However, even under robust DDR conditions, MVM infection did not result in detectable Chk1 phosphorylation. Taken together, these results demonstrated that even in the presence of an activated DDR, the displacement of MVM single-stranded DNA during replication did not induce activated Chk1 in either murine A9 or human 324K cells.

ATR pathway proteins are stable and ATR-ATRIP is recruited to APAR bodies during MVM infection. ATR activation of Chk1 is a multistep process that involves a number of cellular proteins (59), and a number of DNA viruses prevent ATR activation and/or Chk1 phosphorylation by targeting for degradation members of the ATR pathway (60). Immunoblot experiments shown in Fig. 2 demonstrate that this is not the case for MVM infection. Following infection of the human 324K (Fig. 2A) and murine A9 (not shown) cell lines, levels of ATR, ATRIP, Rad17, Rad9, Hus1, and TOPBP1 remained relatively constant (Fig. 2A, compare lanes 2 and 3 with lane 1), although there was a slight reduction in Rad1 levels at 24 h postinfection (hpi) in the experiment shown (Fig. 2A, lane 3). As also shown above, Chk1 phosphorylation was not observed following MVM infection but was detectable following HU treatment (Fig. 2A, compare lane 4 with lanes 2 and 3). Claspin levels were significantly increased upon HU treatment (Fig. 2A, lane 4), likely due to inhibition of its degradation following fork stalling, as has been previously reported (61–65). Taken together, our data suggest that the lack of Chk1 activation during MVM infection did not result from a significant loss of known ATR pathway proteins.

ATRIP senses RPA-associated single-stranded DNA at sites of DNA damage via its conserved C-terminal domain (12). By binding tightly to ATR, ATRIP recruits ATR to RPA-bound single-stranded DNA at DNA damage sites. MVM infection has been shown to induce recruitment of RPA to APAR bodies (31, 37). In addition, many DDR proteins phosphorylated following MVM infection, such as phosphorylated RPA and Chk2, also localize to these same sites (26, 33). Figures 2B and C show redistribution of ATR (Fig. 2B, right panel) and ATRIP (Fig. 2C, right panel) into APAR bodies, as identified by colocalization with NS1, following MVM infection. Redistributed ATR/ATRIP appeared to be chromatin associated, since the signal was resistant to detergent preextraction, which removes soluble, non-chromatin-bound proteins prior to fixation (8). Mock-treated cells showed only background

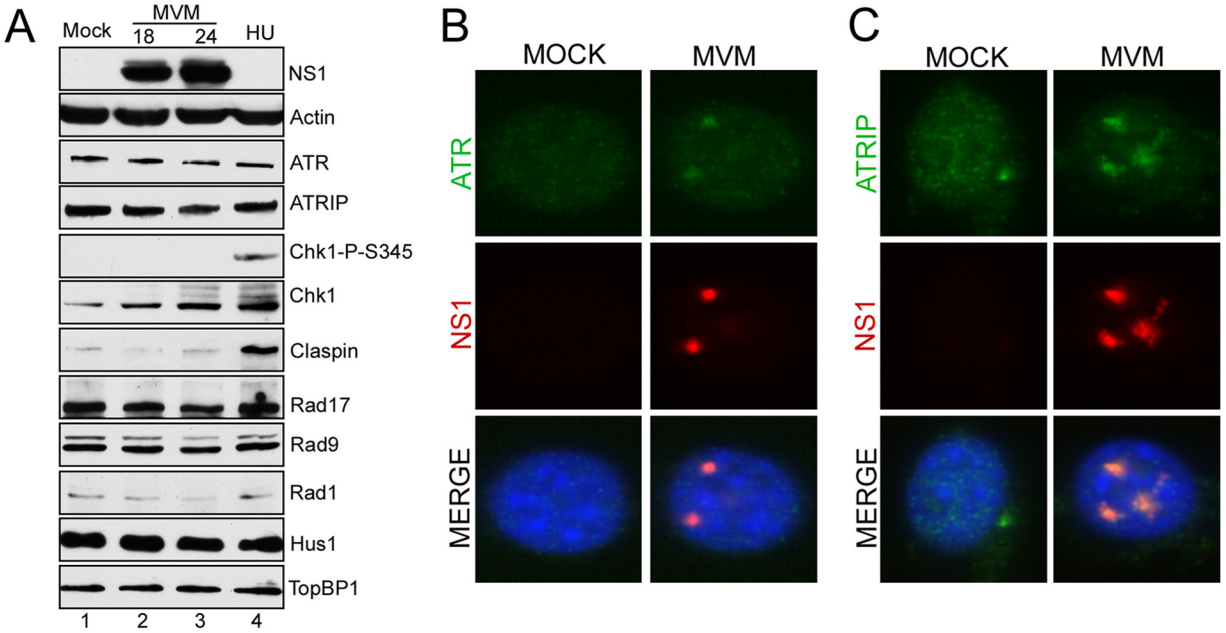

FIG 2 ATR-Chk1 pathway proteins are stable, and ATR/ATRIP is recruited to viral replication bodies. (A) Human 324K cells were infected with MVM at an MOI of 10 for the indicated time points (18 and 24 h). Control cells were treated with 1 mM hydroxyurea (HU) for 12 h. Whole-cell lysates were processed for Western blotting using antibodies directed against the indicated proteins. (B and C) Murine 324K cell lines were infected with MVM at an MOI of 10. Cells were preextracted with cytoskeleton buffer, fixed, and stained using antibodies directed against the indicated proteins. Nuclei were visualized by DAPI staining. Colocalization with NS1 in infected cells with detectable APAR bodies was around 60% (ATR) and 90% (ATRIP).

staining, indicating the lack of association with DNA for ATR/ATRIP in the absence of infection (Fig. 2B and C, left panels). Thus, although Chk1 is not activated by ATR during MVM infection, ATR/ATRIP is recruited to MVM APAR bodies and is presumably associated with DNA at sites of viral replication and accumulation of DNA damage proteins. Whether ATR/ATRIP interacts with viral or cellular DNA has not yet been unequivocally determined.

Unlike ATR-ATRIP, Rad9 is excluded from chromatin at MVM replication compartments. Chk1 activation requires not just ATR/ATRIP loading onto chromatin but also loading of the 9-1-1 clamp onto free 5′ ends of DNA by the Rad17-RFC complex (11, 59). To examine whether known 9-1-1 complex constituents associated with chromatin during MVM infection, we performed chromatin fractionation experiments. The efficacy of our fractionation procedure was confirmed by assaying for the presence or absence of chromatin-associated histone H3 (data not shown), which was then used as a control for equal loading of chromatin-associated proteins (Fig. 3A).

As expected, either infection with MVM or HU treatment resulted in increased amounts of chromatin-associated RPA (Fig. 3A, compare lanes 2 and 3 with lane 1). Altered mobility of RPA in the blot (Fig. 3A, lanes 2 and 3) is presumably indicative of extensive phosphorylation. MVM infection resulted in a marked increase in the slower-migrating form of RPA32 compared to results with HU treatment, consistent with its extensive phosphorylation by various kinases during infection (26, 31). The differences may also reflect potential variations in the DDR between the two conditions, for example, the absence of ATR signaling to RPA during MVM infection, in contrast to results with HU treatment (see also Fig. 6). RPA loading onto single-stranded DNA is a potent trigger for recruitment of ATR-ATRIP, and consequently we observed increased chromatin association of ATR in infected cells (Fig. 3A, compare lanes 1 and 2). This finding was consistent with our previous observation of increased ATR/ATRIP loading onto DNA at or near APAR bodies following immunofluorescence (Fig. 2B). Loading of the 9-1-1 complex occurs independently of ATR-ATRIP loading, and both events are required for efficient Chk1 activation (11, 59). Although total levels of Rad9 were not diminished following MVM infection (Fig. 2A and data not shown), we consistently detected reduced chromatin association of Rad9 during infection (Fig. 3A, lane 2). Under these conditions, the low levels of Rad9 present appeared to migrate faster, possibly due to reduced phosphorylation. In contrast, HU treatment resulted in a slight increase in Rad9 association with chromatin (Fig. 3A, lane 3), as has been found previously with other genotoxic agents (66, 67).

We also examined localization of these proteins and potential association with chromatin by immunofluorescence. MVM-infected 324K cells were preextracted to remove non-chromatin-associated proteins and probed for RPA and Rad9. Control cells were treated with HU. Similar to the results obtained by Western blotting, we detected increased amounts of detergent-resistant RPA following MVM infection which colocalized with NS1 at viral replication compartments in the nucleus (Fig. 3B). HU treatment also led to increased chromatin association of RPA at foci distributed throughout the nucleus (Fig. 3B). In contrast, while HU treatment resulted in increased chromatin association of Rad9 at foci distributed throughout the nucleus, neither mock infection nor MVM infection led to an increase in the association of Rad9 with chromatin (Fig. 3B). Thus, during MVM infection and unlike ATR/ATRIP, Rad9, an essential component of the 9-1-1 complex, was not efficiently loaded onto chromatin, which could explain why Chk1 was not activated during MVM infection.

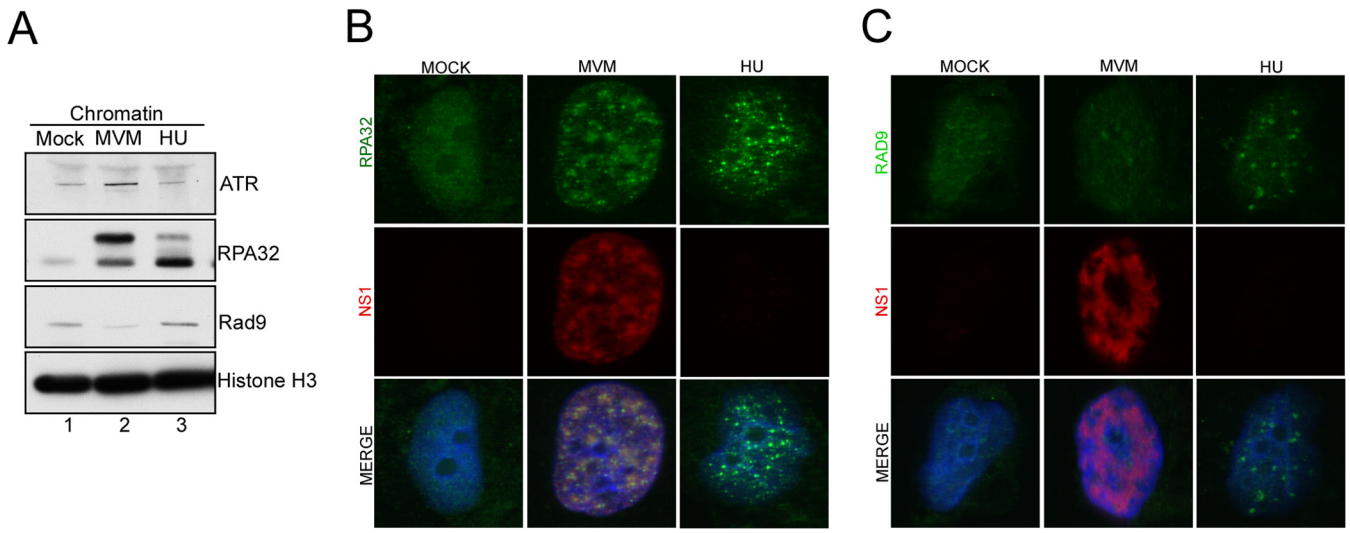

FIG 3 Rad9 does not efficiently associate with chromatin during MVM infection. (A) Human 324K cells were infected with MVM at an MOI of 10 for 24 h. Control cells were treated with 1 mM HU for 6 h. Cells were harvested and fractionated as described in Materials and Methods, and 2% SDS lysates of the chromatin fraction were assayed by Western blotting using antibodies directed against the indicated proteins. (B and C) Human 324K cells were infected with MVM at an MOI of 10 for 24 h. Control cells were treated with 1 mM hydroxyurea (HU) for 12 h. Cells were preextracted with cytoskeleton buffer, fixed, and stained using antibodies directed against the indicated proteins. Nuclei were stained with DAPI.

Whether the virus actively mislocalizes Rad9 or whether it is merely a consequence of the absence of exposed 5′ DNA ends in viral replication compartments is currently being investigated.

Stalling of MVM replication early in infection triggers Chk1 phosphorylation. Having shown that Chk1 was not phosphorylated during MVM infection, we performed time course experiments (data not shown) to determine whether MVM infection affected Chk1 activation in response to agents that stall replication forks and are known to induce ATR-Chk1 activation. As mentioned previously, HU treatment depletes deoxynucleoside triphosphates (dNTPs) from cells, causing cellular replication forks/complexes to stall (44). Consistent with its role in inhibiting cellular replication fork progression and the known reliance of MVM on host polymerases for its replication, we have found that treatment of MVM-infected cells with HU inhibits progression of MVM replication (data not shown). Surprisingly, treatment of infected cells with HU at early time points (15 h to 18 h) following infection resulted in a marked increase in Chk1 phosphorylation compared to that for mock-infected cells (Fig. 4A, compare lanes 2 and 4). This effect was not seen at later time points (see Fig. 5; described below). Similar results are also apparent as part of the experiment shown in Fig. 4B (Fig. 4B, lanes 1 to 4). The low levels of Chk1 phosphorylation following HU treatment of mock-infected cells (Fig. 4A, lane 2, and B, lane 2) was likely due to the paucity of active cellular replication forks this early in S phase, since at 15 h postrelease (hpr) of this particular block (at which time HU was added), cells are at the beginning of S phase (33). In addition, extensive time course experiments have shown that at this early time point in this particular blocking protocol, viral replication was just beginning ([33]; also data not shown). In our previous work, we have demonstrated that viral replication is required for detectable DDR signaling (26). There was low but detectable NS1 expression in these experiments (Fig. 4B, lanes 3 and 4), but since replication had not fully commenced at this point, there was no detectable DNA-damaging signaling (Fig. 4B, lane 3; note the absence of RPA phosphorylation in infected cells not treated with HU; compare with Fig. 1B, lane 2). Taken together, these results suggested that at early times postinfection, prior to full virally induced DDR signaling, MVM-infected cells could be artificially induced to activate Chk1 following treatment which HU.

To determine whether the marked increase in Chk1 phosphorylation at these times was a response to the blocking by HU of the extension of self-primed, viral replicating strands or was merely due to the incoming viral genomes, we infected cells with UV-treated MVM (UV-MVM). We have previously demonstrated that UV-treated virus under these conditions failed to express NS1 and did not replicate (26) (note the absence of NS1 expression in Fig. 4B, lanes 5 and 6). Treatment of cells with UV-MVM alone did not cause Chk1 phosphorylation (Fig. 4B, lane 5), and consistent with a requirement for replication-competent virus, UV-MVM, unlike wild-type virus, failed to induce a similar increase in Chk1 phosphorylation upon treatment with HU (Fig. 4B, compare lanes 3 and 6). Thus, only MVM molecules that were competent in assembling replication proteins/complexes and/or initiating viral replication could trigger Chk1 phosphorylation following HU treatment. It should be noted that full viral replication was not required for this event, since (i) viral replication was just beginning at this time point, and (ii) HU treatment (as well as aphidicolin treatment; see below) inhibits MVM replication. Under these conditions, HU-induced RPA32 phosphorylation during infection was not increased compared to results with HU treatment of mock-infected cells (Fig. 4B, compare lanes 2 and 3). This was likely because S4/8 is mainly phosphorylated by DNA PK (68, 69), which does not require long stretches of RPA on stalled replication forks for its activation, consistent with the model that it is this structure that is formed following HU treatment of MVM-infected cells. Additionally, we also observed that increasing the MVM MOI resulted in a dose-dependent increase in Chk1 phosphorylation following HU treatment at this early time point

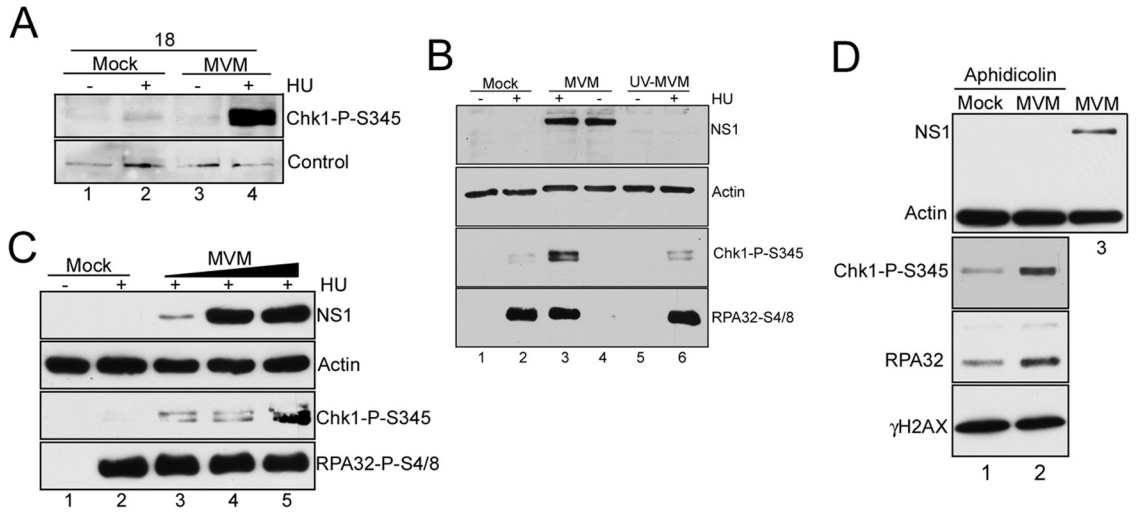

FIG 4 Stalling of MVM replication "forks" early in infection triggers Chk1 phosphorylation. (A) Murine A9 cells were parasynchronized by isoleucine deprivation and infected with MVM at an MOI of 10 at the time of release into complete medium. At 15 hpr, cells were treated with 3 mM HU or vehicle control for 3 h and harvested at 18 hpr. RIPA lysates were quantitated by Bradford assay, and equal protein amounts were loaded in wells and processed for Western blotting using antibodies directed against phospho-Chk1. "Control" is a nonspecific band that served as a control for loading. (B) Murine A9 cells were treated as described above for Fig. 3A. Cells were infected with wild-type MVM or UV-inactivated virus and processed by Western blotting using antibodies directed against the indicated proteins. (C) Murine A9 cells treated as described for Fig. 3A were infected with increasing MOIs of MVM (0.1, 1, and 10). Cells were processed for Western blotting using antibodies directed against the indicated proteins. (D) Murine A9 cells were parasynchronized by isoleucine deprivation and then released into medium containing aphidicolin for an additional 16 h to achieve a tight synchronization at the G_1/S border. Infection with MVM at an MOI of 10 was performed at the time of release into medium containing aphidicolin. Control cells are shown in lane 3 to demonstrate the absence of NS1 expression in aphidicolin-treated cells in lanes 1 and 2. These cells were released into aphidicolin-free medium after isoleucine block and harvested at 18 h to allow progression into S phase and expression of NS1. Cell lysates were processed for Western blotting using antibodies directed against the indicated proteins.

(Fig. 4C), further suggesting an association with available yet stalled viral replication strands/complexes.

In the experiments described above, since there was detectable NS1 expression, we could not rule out a role for NS1 in triggering Chk1 phosphorylation following HU treatment. Similarly, we could not rule out that this phenotype was an artifact of HU treatment independent of the stalling of polymerase on viral replication strands. Thus, in a complementary set of experiments, we examined induction of Chk1 activation during the early stages of MVM infection following treatment with aphidicolin. Aphidicolin also leads to stalling of replication complexes but via a different mechanism than that of HU; it directly inhibits extension of DNA polymerase, leading to cell cycle arrest at early G_1/S phase (70, 71). Murine A9 cells were blocked by isoleucine deprivation as before, released directly into medium containing low doses of aphidicolin, and either mock treated or infected with an MOI of MVM similar to that used above. This protocol is similar to the "double-block" procedure which has been used extensively to study MVM replicative forms (40, 72). Addition of aphidicolin for the entirety of the infection period prevented initiation of MVM replication and, as expected, MVM-infected cells failed to express NS1 under these conditions (see Fig. 4D, lane 2; an additional lane not treated with aphidicolin was added for reference in lane 3). Similar to results with HU, we observed Chk1 phosphorylation in MVM-infected cells that was increased over that in mock-infected cells (Fig. 4D, compare lanes 1 and 2). Total RPA32 levels were also increased for reasons not yet clear; however, overall DDR signaling in response to aphidicolin treatment (as evidenced by H2AX phosphorylation) was similar under the two conditions. We note that within 4 h after release from the aphidicolin block, viral replication resumed/commenced, and both Chk1 and H2AX phosphorylation was lost (data not shown), demonstrating the reversible effect of aphidicolin on viral replication complexes. Taken together, our results suggest that primed, replication-competent viral molecules could trigger Chk1 phosphorylation upon "fork" or replicating strand stalling independently of NS1 expression and viral replication.

Full MVM infection prevents ATR-Chk1 signaling in response to exogenous DNA-damaging agents. In contrast to what was observed very early after infection, HU treatment 21 to 24 hpr of parasynchronized MVM-infected cells resulted in reduced activation of Chk1 (Fig. 5A, lane 4). Under these conditions, HU treatment resulted in a marked increase in Chk1 phosphorylation in uninfected cells (Fig. 5A, lane 2).

Although MVM induces a DDR which leads to cell cycle arrest in G_2 phase, it is unlikely that the reduction in Chk1 activation in infected cells compared to that in mock-infected cells was due merely to reduction in the S-phase population. By 21 to 24 hpi, when infected cells are arrested in G_2 phase and cellular replication has effectively ceased, viral genomes continue to actively replicate (26, 33, 73–75). And having shown that stalling of the replicative polymerase on MVM genomes can induce ATR-Chk1 signaling (Fig. 4), our data suggest that unlike the case early in infection, prior to establishment of full viral replication and detectable DNA damage signaling, stalling of MVM replication complexes by HU at late time points postinfection was not sufficient to induce Chk1 activation.

To determine whether MVM inhibition of HU activation of Chk1 at late times during infection was an active process and independent of the type of ATR activating signal, we examined whether full MVM infection could prevent Chk1 signaling in response to other genotoxic agents which do not activate ATR via

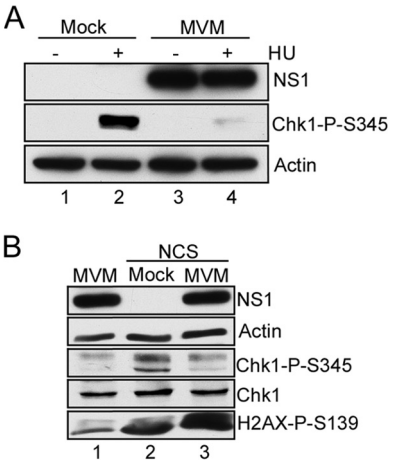

FIG 5 Full MVM infection prevents ATR-Chk1 phosphorylation in response to exogenous DNA-damaging agents. (A) Parasynchronized murine A9 cells were released into complete medium and infected with MVM at an MOI of 10 at the time of release. At 24 hpr, cells were treated with 3 mM HU or vehicle control for 3 h. RIPA lysates were processed for Western blotting using antibodies directed against the indicated proteins. (B) Parasynchronized murine A9 cells were released into complete medium and infected with MVM at an MOI of 10 at the time of release. At 24 hpr, cells were treated with 150 ng/ml of NCS for 1 h. Cells were harvested and processed for Western blotting using antibodies directed against the indicated proteins.

stalling of replication forks. Thus, experiments similar to those described above were performed using NCS, which, as mentioned above, induces DSBs in chromatin, leading to ATM activation. Processing and resection of DSBs results in subsequent ATR signaling, which can take place both during S and G_2 phases. Thus, as with ionizing radiation treatment, a G_2 block does not prevent induction of Chk1 activation by NCS (55, 58). Treatment of mock-infected cells with NCS 24 to 25 hpr led to increased phosphorylation of Chk1 (Fig. 5B, lane 2); however, similar treatment of MVM-infected (and also G_2-arrested) cells also resulted in reduced Chk1 activation (Fig. 5B, lane 3). Interestingly, NCS treatment under these conditions led to increased H2AX phosphorylation (a marker of DSB formation [48, 76]) in both mock-infected and MVM-infected cells (Fig. 5B, compare lanes 2 and 3 with lane 1), suggesting that MVM infection blocks ATR-Chk1 signaling by NCS at a point after induction of DSBs. Thus, the prevention of Chk1 activation by MVM was not due simply to the inhibition of cellular DNA replication or restricted to triggering due to stalled replication forks. Taken together, our data suggest that upon onset of full viral replication, MVM blocks Chk1 activation triggered by diverse stimuli.

Activation status of ATR following MVM infection. In addition to Chk1, ATR is known to phosphorylate a number of other proteins following its activation (11). In particular, phosphorylation of RPA32 serine 33 (S33) has been attributed to ATR activity (77, 78). Phosphorylation of RPA32 on S33 in response to MVM infection has been reported by others (31). Therefore, we performed siRNA knockdown experiments (Fig. 6A) and drug inhibition experiments (Fig. 6B) to determine whether ATR was involved in this phosphorylation event in infected cells. In repeated experiments, we failed to observe a decrease in RPA32 phosphorylation on S33 following depletion of ATR by either siRNA (Fig. 6A, compare lanes 2 and 3 with lane 1) or inhibition of ATR using a recently reported, highly potent ATR inhibitor (79, 80) (Fig. 6B, compare lanes 2 and 3 with lane 1). Similar results were observed in MVM-infected murine A9 cells following ATR depletion by siRNA (data not shown). Taken together, these results suggest that ATR may not be required for phosphorylation of RPA32 during MVM infection. Exactly how RPA32 is phosphorylated at S33 during MVM infection is under investigation.

ATM and DNA PK have well-characterized autophosphorylation sites which serve as markers for their activation (81, 82). Recently, a similar autophosphorylation event on threonine 1989 (T1989) in human cells which correlates with ATR activation was identified (43, 83). The site is not well conserved across mammalian species, and the detailed role this phosphorylation plays in ATR downstream signaling remains unclear. As has been previously reported (43, 83), HU treatment resulted in marked phosphorylation of ATR at T1989 (Fig. 6C, lane 4). At 18 h following MVM infection, there was slight but detectable phosphorylation of ATR at this site; however, by 24 hpi, phosphorylation of ATR at T1989 was undetectable (Fig. 6C, lanes 2 and 3). As also mentioned above, there was an increase of total ATR immunoprecipitable from the chromatin fraction of both MVM-infected and HU-treated 324K cells (Fig. 6C, lanes 2, 3, and 4), while mock-treated cells displayed little ATR association with chromatin (Fig. 6C, lane 1). Thus, during MVM infection, even though there was an increase in total ATR associated with chromatin, either it failed to be autophosphorylated at T1989 or its phosphorylation could not be maintained.

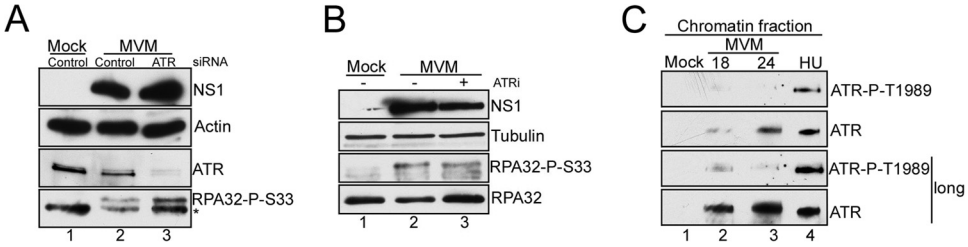

FIG 6 Activation status of ATR and its role in MVM DDR signaling. (A) Human 324K cells were transfected twice with control siRNA or siRNA directed against ATR as indicated. Sixteen hours after the second transfection, cells were either mock infected or infected with MVM at an MOI of 10. Twenty-four hours later, cells were processed for Western blotting using antibodies directed against the indicated proteins. "*" indicates a nonspecific band. (B) Human 324K cells were infected with MVM at an MOI of 10 as indicated. Eight hours after infection, cells were treated with 10 μM ATR inhibitor (ATRi) for 16 h. Cells were harvested 24 hpi and processed for Western blotting using antibodies against the indicated proteins. (C) Human 324K cells were infected with MVM at an MOI of 10 for the indicated time periods. Control cells were treated with HU as described above. Cells were fractionated as described above, and ATR was immunoprecipitated from the chromatin fraction. Western blotting analyses were performed using antibodies directed against the indicated proteins.

DISCUSSION

ATM and ATR are the major kinases that coordinate the DNA damage response to diverse DNA damage stimuli (1). Although a significant amount has been discovered about ATM activation during parvoviral infection, involvement of the ATR pathway has not been investigated in detail. An important point in this regard is that during MVM infection, Chk1, a major downstream target of ATR, is not detectably phosphorylated. In this report, we demonstrate that MVM replication was sufficient to induce recruitment and retention of ATR/ATRIP into viral replication centers (APAR bodies). ATR and ATRIP were associated with chromatin upon fractionation; whether the association is to viral DNA, cellular DNA, or both is under investigation. Such relocalization was not surprising, because ATRIP binds to RPA, bulk RPA is known to be redistributed to APAR bodies, and in this article we have shown that redistributed RPA is chromatin associated. However, Rad9, an integral component of the 9-1-1 complex, was not loaded onto chromatin. Absence of Rad9 loading onto chromatin could fully account for a failure to activate Chk1.

A similar mechanism involving failure to recruit the 9-1-1 complex was recently reported to occur during herpes simplex virus 1 (HSV-1) infection (84). In this case, the viral single-stranded DNA binding protein (ICP8) and the helicase/primase complex (UL8/UL5/UL52) compete with the 9-1-1 complex for binding to free 5′ DNA. Rad9 is essential for recruitment of the ATR activator TOPBP1, and in preliminary experiments, we could not detect TOPBP1 association with chromatin fractions (data not shown). Exactly why Rad9 is not recruited is not clear. Rad9 is loaded onto primer-template junctions with exposed 5′ ends (13, 14, 85). This structure is commonly found at lagging strands and would require a repriming event to occur on leading strands (11, 59). If parvovirus replicating DNA is the primary source of the virus-induced DDR, it may fail to generate exposed 5′ ends at stalled forks because its single-stranded genome undergoes a leading-strand displacement, rolling-circle-type replication (73, 86). If this were the case, all parvoviruses should fail to induce Chk1 activation; however, parvovirus B19 and minute virus of canines (MVC) have been reported to do so (30, 87). During MVM replication and likely for the replication of other parvoviruses, the viral replicator protein NS1 nicks replicating viral genomes during maturation to generate 5′ ends (73, 86). For MVM, this structure may not be "exposed," since NS1 remains attached to the 5′ end of the nicked site (72). Binding of NS1 to the 5′ ends of MVM genomes might be an active way of preventing recognition of free 5′ ends in a manner effectively similar to that of the four-protein complex of HSV-1 (84), and perhaps this does not occur for MVC and B19. Whether this is the case or not is under investigation.

While we did not observe Chk1 phosphorylation under native infection conditions, we surprisingly found that treatment of infected cells with agents that stall replication forks can trigger marked Chk1 phosphorylation. This mimicking of a stalled-replication fork is reminiscent of a previously reported event seen following infection with UV-AAV (29). This effect was only seen very early during infection of para-synchronized cells, at a time when the cells were in early S phase. At this time, treatment of mock-infected cells with hydroxyurea did not induce significant Chk1 phosphorylation presumably because very few cellular replication origins had fired. The phosphorylation event in infected cells was not due to direct effects of NS1, but did require replication-competent virus. This was in contrast to the previous observations with UV-treated adeno-associated virus (AAV); in our case, UV-MVM was unable to induce Chk1 activation by itself or in the presence of HU. The reasons for these differences are not clear. Remarkably, upon full viral infection and replication at later times during infection, not only did we fail to see the marked increase in Chk1 phosphorylation but it was reduced compared to results with control cells treated with various DNA-damaging drugs. This suggested not only that MVM failed to activate Chk1 but also that there may have been an active mechanism in place for preventing such phosphorylation events in infected cells. Whether that mechanism is manifested via a mechanism related to the prevention of the association of Rad9 with chromatin is not yet clear. One of the differences between the situation early in infection versus late was that although infected cells had transited into S phase early (there was detectable NS1 expression), there was no DDR signaling apparent at the early time point. At late time points during infection, the virally induced DDR was robust. Progression and maturation of APAR bodies during MVM replication and the MVM-induced DDR response involve recruitment and accumulation of large amounts of DNA repair proteins at these sites (26, 31, 37). It may be that sequestration of DDR and repair factors at replication factories actively prevented activation of Chk1 in response to exogenous DNA-damaging agents.

ATR itself was not found to be autophosphorylated on T1989 at late times following MVM infection. Similar observations were previously reported when examining phosphor-ATR S428 (31); however, a correlation between S428 phosphorylation and ATR activity has recently been questioned (83). Tellingly, we have found that phosphorylation of RPA32 S33, which is associated with ATR activity following several drug treatments (77, 78), was not affected by ATR inhibition during MVM infection. Thus, ATR was also unlikely to be active in phosphorylating targets other than Chk1 during infection. Although Rad9 and TOPBP1 are required for full ATR signaling, neither protein is essential for the autophosphorylation event that marks active ATR (43). Thus, the absence of phosphorylated ATR could not be explained simply by the failure to load Rad9 onto DNA. For reasons not yet clear, we did observe low levels of phosphorylated ATR early during infection, which was lost as the infection progressed. That introduction of viral DNA triggers a transient activation of ATR that is not sustained due to the absence of downstream Chk1 signaling has not been ruled out.

A number of viruses inactivate ATR signaling during infection, including papillomaviruses (88), adenoviruses (89, 90), Epstein-Barr virus (EBV) (91), HSV-1 (84, 92), and others (60, 93), and they employ varied mechanisms to do so. For example, adenovirus 12 inactivates ATR signaling by targeting TOPBP1 for degradation (89), and adenovirus 5 E4 oncoproteins target the MRN complex for degradation and/or mislocalization to prevent ATM/ATR activation (90, 94). The viral benefits for inhibition of ATR activity during infection are not fully clear. ATR possesses a number of activities that might be detrimental to viral replication, including inhibition of CDK activity, inhibition of new origin firing, induction of cell cycle checkpoints, and promotion of homologous recombination repair (11, 95). Conversely, ATR activity has been suggested to be important for efficient parvovirus B19 infection (87), and although HSV-1 inactivates ATR/Chk1 activation, it still requires ATR and ATR pathway proteins for efficient repli-

cation (96). Why the ATR signaling pathway is not activated during MVM infection is under investigation. Since ATR/ATRIP is recruited to MVM replication compartments, it would be interesting to determine whether ATR might play a structural role at those sites during MVM infection and to investigate potential inhibitory effects of ATR kinase or Chk1 kinase activity.

ACKNOWLEDGMENTS

This work was supported by Public Health Service grants AI-046458 and AI-091588 from NIAID.

We thank members of the Pintel lab for helpful advice and discussions and Lisa Burger for expert technical assistance.

REFERENCES

1. **Ciccia A, Elledge SJ.** 2010. The DNA damage response: making it safe to play with knives. Mol. Cell **40:**179–204. http://dx.doi.org/10.1016/j.molcel.2010.09.019.
2. **Jackson SP, Bartek J.** 2009. The DNA-damage response in human biology and disease. Nature **461:**1071–1078. http://dx.doi.org/10.1038/nature08467.
3. **Polo SE, Jackson SP.** 2011. Dynamics of DNA damage response proteins at DNA breaks: a focus on protein modifications. Genes Dev. **25:**409–433. http://dx.doi.org/10.1101/gad.2021311.
4. **Jackson SP, Durocher D.** 2013. Regulation of DNA damage responses by ubiquitin and SUMO. Mol. Cell **49:**795–807. http://dx.doi.org/10.1016/j.molcel.2013.01.017.
5. **Abraham RT.** 2004. PI 3-kinase related kinases: 'big' players in stress-induced signaling pathways. DNA Repair **3:**883–887. http://dx.doi.org/10.1016/j.dnarep.2004.04.002.
6. **Durocher D, Jackson SP.** 2001. DNA-PK, ATM and ATR as sensors of DNA damage: variations on a theme? Curr. Opin. Cell Biol. **13:**225–231. http://dx.doi.org/10.1016/S0955-0674(00)00201-5.
7. **Falck J, Coates J, Jackson SP.** 2005. Conserved modes of recruitment of ATM, ATR and DNA-PKcs to sites of DNA damage. Nature **434:**605–611. http://dx.doi.org/10.1038/nature03442.
8. **Sowd GA, Li NY, Fanning E.** 2013. ATM and ATR activities maintain replication fork integrity during SV40 chromatin replication. PLoS Pathog. **9:**e1003283. http://dx.doi.org/10.1371/journal.ppat.1003283.
9. **Stiff T, O'Driscoll M, Rief N, Iwabuchi K, Lobrich M, Jeggo PA.** 2004. ATM and DNA-PK function redundantly to phosphorylate H2AX after exposure to ionizing radiation. Cancer Res. **64:**2390–2396. http://dx.doi.org/10.1158/0008-5472.CAN-03-3207.
10. **Brown EJ, Baltimore D.** 2000. ATR disruption leads to chromosomal fragmentation and early embryonic lethality. Genes Dev. **14:**397–402.
11. **Cimprich KA, Cortez D.** 2008. ATR: an essential regulator of genome integrity. Nat. Rev. Mol. Cell. Biol. **9:**616–627. http://dx.doi.org/10.1038/nrm2450.
12. **Zou L, Elledge SJ.** 2003. Sensing DNA damage through ATRIP recognition of RPA-ssDNA complexes. Science **300:**1542–1548. http://dx.doi.org/10.1126/science.1083430.
13. **Bermudez VP, Lindsey-Boltz LA, Cesare AJ, Maniwa Y, Griffith JD, Hurwitz J, Sancar A.** 2003. Loading of the human 9-1-1 checkpoint complex onto DNA by the checkpoint clamp loader hRad17-replication factor C complex in vitro. Proc. Natl. Acad. Sci. U. S. A. **100:**1633–1638. http://dx.doi.org/10.1073/pnas.0437927100.
14. **Ellison V, Stillman B.** 2003. Biochemical characterization of DNA damage checkpoint complexes: clamp loader and clamp complexes with specificity for 5′ recessed DNA. PLoS Biol. **1:**E33. http://dx.doi.org/10.1371/journal.pbio.0000033.
15. **Zou L, Liu D, Elledge SJ.** 2003. Replication protein A-mediated recruitment and activation of Rad17 complexes. Proc. Natl. Acad. Sci. U. S. A. **100:**13827–13832. http://dx.doi.org/10.1073/pnas.2336100100.
16. **Delacroix S, Wagner JM, Kobayashi M, Yamamoto K, Karnitz LM.** 2007. The Rad9-Hus1-Rad1 (9-1-1) clamp activates checkpoint signaling via TopBP1. Genes Dev. **21:**1472–1477. http://dx.doi.org/10.1101/gad.1547007.
17. **Kumagai A, Lee J, Yoo HY, Dunphy WG.** 2006. TopBP1 activates the ATR-ATRIP complex. Cell **124:**943–955. http://dx.doi.org/10.1016/j.cell.2005.12.041.
18. **Duursma AM, Driscoll R, Elias JE, Cimprich KA.** 2013. A role for the MRN complex in ATR activation via TOPBP1 recruitment. Mol. Cell **50:**116–122. http://dx.doi.org/10.1016/j.molcel.2013.03.006.
19. **Lee J, Dunphy WG.** 2013. The Mre11-Rad50-Nbs1 (MRN) complex has a specific role in the activation of Chk1 in response to stalled replication forks. Mol. Biol. Cell **24:**1343–1353. http://dx.doi.org/10.1091/mbc.E13-01-0025.
20. **Kumagai A, Dunphy WG.** 2000. Claspin, a novel protein required for the activation of Chk1 during a DNA replication checkpoint response in Xenopus egg extracts. Mol. Cell **6:**839–849. http://dx.doi.org/10.1016/S1097-2765(05)00092-4.
21. **Liu S, Bekker-Jensen S, Mailand N, Lukas C, Bartek J, Lukas J.** 2006. Claspin operates downstream of TopBP1 to direct ATR signaling towards Chk1 activation. Mol. Cell. Biol. **26:**6056–6064. http://dx.doi.org/10.1128/MCB.00492-06.
22. **Liu S, Song N, Zou L.** 2012. The conserved C terminus of Claspin interacts with Rad9 and promotes rapid activation of Chk1. Cell Cycle **11:**2711–2716. http://dx.doi.org/10.4161/cc.21041.
23. **Wang X, Zou L, Lu T, Bao S, Hurov KE, Hittelman WN, Elledge SJ, Li L.** 2006. Rad17 phosphorylation is required for claspin recruitment and Chk1 activation in response to replication stress. Mol. Cell **23:**331–341. http://dx.doi.org/10.1016/j.molcel.2006.06.022.
24. **Liu Q, Guntuku S, Cui XS, Matsuoka S, Cortez D, Tamai K, Luo G, Carattini-Rivera S, DeMayo F, Bradley A, Donehower LA, Elledge SJ.** 2000. Chk1 is an essential kinase that is regulated by Atr and required for the G(2)/M DNA damage checkpoint. Genes Dev. **14:**1448–1459.
25. **Zhao H, Piwnica-Worms H.** 2001. ATR-mediated checkpoint pathways regulate phosphorylation and activation of human Chk1. Mol. Cell. Biol. **21:**4129–4139. http://dx.doi.org/10.1128/MCB.21.13.4129-4139.2001.
26. **Adeyemi RO, Landry S, Davis ME, Weitzman MD, Pintel DJ.** 2010. Parvovirus minute virus of mice induces a DNA damage response that facilitates viral replication. PLoS Pathog. **6:**e1001141. http://dx.doi.org/10.1371/journal.ppat.1001141.
27. **Adeyemi RO, Pintel DJ.** 2012. Replication of minute virus of mice in murine cells is facilitated by virally induced depletion of p21. J. Virol. **86:**8328–8332. http://dx.doi.org/10.1128/JVI.00820-12.
28. **Cotmore SF, Tattersall P.** 2013. Parvovirus diversity and DNA damage responses. Cold Spring Harb Perspect Biol. **5:**a012989. http://dx.doi.org/10.1101/cshperspect.a012989.
29. **Jurvansuu J, Raj K, Stasiak A, Beard P.** 2005. Viral transport of DNA damage that mimics a stalled replication fork. J. Virol. **79:**569–580. http://dx.doi.org/10.1128/JVI.79.1.569-580.2005.
30. **Luo Y, Chen AY, Qiu J.** 2011. Bocavirus infection induces a DNA damage response that facilitates viral DNA replication and mediates cell death. J. Virol. **85:**133–145. http://dx.doi.org/10.1128/JVI.01534-10.
31. **Ruiz Z, Mihaylov IS, Cotmore SF, Tattersall P.** 2011. Recruitment of DNA replication and damage response proteins to viral replication centers during infection with NS2 mutants of Minute Virus of Mice (MVM). Virology **410:**375–384. http://dx.doi.org/10.1016/j.virol.2010.12.009.
32. **Schwartz RA, Carson CT, Schuberth C, Weitzman MD.** 2009. Adeno-associated virus replication induces a DNA damage response coordinated by DNA-dependent protein kinase. J. Virol. **83:**6269–6278. http://dx.doi.org/10.1128/JVI.00318-09.
33. **Adeyemi RO, Pintel DJ.** 2014. Parvovirus-induced depletion of cyclin B1 prevents mitotic entry of infected cells. PLoS Pathog. **10:**e1003891. http://dx.doi.org/10.1371/journal.ppat.1003891.
34. **Chen AY, Luo Y, Cheng F, Sun Y, Qiu J.** 2010. Bocavirus infection induces mitochondrion-mediated apoptosis and cell cycle arrest at G2/M phase. J. Virol. **84:**5615–5626. http://dx.doi.org/10.1128/JVI.02094-09.
35. **Chen AY, Qiu J.** 2010. Parvovirus infection-induced cell death and cell cycle arrest. Future Virol. **5:**731–743. http://dx.doi.org/10.2217/fvl.10.56.
36. **Luo Y, Deng X, Cheng F, Li Y, Qiu J.** 2013. SMC1-mediated intra-S-phase arrest facilitates bocavirus DNA replication. J. Virol. **87:**4017–4032. http://dx.doi.org/10.1128/JVI.03396-12.
37. **Bashir T, Rommelaere J, Cziepluch C.** 2001. In vivo accumulation of cyclin A and cellular replication factors in autonomous parvovirus minute virus of mice-associated replication bodies. J. Virol. **75:**4394–4398. http://dx.doi.org/10.1128/JVI.75.9.4394-4398.2001.
38. **Cziepluch C, Lampel S, Grewenig A, Grund C, Lichter P, Rommelaere J.** 2000. H-1 parvovirus-associated replication bodies: a distinct virus-induced nuclear structure. J. Virol. **74:**4807–4815. http://dx.doi.org/10.1128/JVI.74.10.4807-4815.2000.
39. **Adeyemi RO, Fuller MS, Pintel DJ.** 2014. Efficient parvovirus replication requires CRL4Cdt2-targeted depletion of p21 to prevent its inhibitory interaction with PCNA. PLoS Pathog. **10:**e1004055. http://dx.doi.org/10.1371/journal.ppat.1004055.

40. **Schoborg RV, Pintel DJ.** 1991. Accumulation of MVM gene products is differentially regulated by transcription initiation, RNA processing and protein stability. Virology **181:**22–34. http://dx.doi.org/10.1016/0042-6822(91)90466-O.
41. **Mendez J, Stillman B.** 2000. Chromatin association of human origin recognition complex, cdc6, and minichromosome maintenance proteins during the cell cycle: assembly of prereplication complexes in late mitosis. Mol. Cell. Biol. **20:**8602–8612. http://dx.doi.org/10.1128/MCB.20.22.8602-8612.2000.
42. **Wysocka J, Reilly PT, Herr W.** 2001. Loss of HCF-1–chromatin association precedes temperature-induced growth arrest of tsBN67 cells. Mol. Cell. Biol. **21:**3820–3829. http://dx.doi.org/10.1128/MCB.21.11.3820-3829.2001.
43. **Liu S, Shiotani B, Lahiri M, Marechal A, Tse A, Leung CC, Glover JN, Yang XH, Zou L.** 2011. ATR autophosphorylation as a molecular switch for checkpoint activation. Mol. Cell **43:**192–202. http://dx.doi.org/10.1016/j.molcel.2011.06.019.
44. **Krakoff IH, Brown NC, Reichard P.** 1968. Inhibition of ribonucleoside diphosphate reductase by hydroxyurea. Cancer Res. **28:**1559–1565.
45. **Huh J, Piwnica-Worms H.** 2013. CRL4(CDT2) targets CHK1 for PCNA-independent destruction. Mol. Cell. Biol. **33:**213–226. http://dx.doi.org/10.1128/MCB.00847-12.
46. **Leung-Pineda V, Huh J, Piwnica-Worms H.** 2009. DDB1 targets Chk1 to the Cul4 E3 ligase complex in normal cycling cells and in cells experiencing replication stress. Cancer Res. **69:**2630–2637. http://dx.doi.org/10.1158/0008-5472.CAN-08-3382.
47. **Zhang YW, Otterness DM, Chiang GG, Xie W, Liu YC, Mercurio F, Abraham RT.** 2005. Genotoxic stress targets human Chk1 for degradation by the ubiquitin-proteasome pathway. Mol. Cell **19:**607–618. http://dx.doi.org/10.1016/j.molcel.2005.07.019.
48. **Burma S, Chen BP, Murphy M, Kurimasa A, Chen DJ.** 2001. ATM phosphorylates histone H2AX in response to DNA double-strand breaks. J. Biol. Chem. **276:**42462–42467. http://dx.doi.org/10.1074/jbc.C100466200.
49. **Lee JH, Paull TT.** 2005. ATM activation by DNA double-strand breaks through the Mre11-Rad50-Nbs1 complex. Science **308:**551–554. http://dx.doi.org/10.1126/science.1108297.
50. **Garcia-Muse T, Boulton SJ.** 2005. Distinct modes of ATR activation after replication stress and DNA double-strand breaks in Caenorhabditis elegans. EMBO J. **24:**4345–4355. http://dx.doi.org/10.1038/sj.emboj.7600896.
51. **Sartori AA, Lukas C, Coates J, Mistrik M, Fu S, Bartek J, Baer R, Lukas J, Jackson SP.** 2007. Human CtIP promotes DNA end resection. Nature **450:**509–514. http://dx.doi.org/10.1038/nature06337.
52. **Takeda S, Nakamura K, Taniguchi Y, Paull TT.** 2007. Ctp1/CtIP and the MRN complex collaborate in the initial steps of homologous recombination. Mol. Cell **28:**351–352. http://dx.doi.org/10.1016/j.molcel.2007.10.016.
53. **Shiotani B, Zou L.** 2009. Single-stranded DNA orchestrates an ATM-to-ATR switch at DNA breaks. Mol. Cell **33:**547–558. http://dx.doi.org/10.1016/j.molcel.2009.01.024.
54. **Cuadrado M, Martinez-Pastor B, Murga M, Toledo LI, Gutierrez-Martinez P, Lopez E, Fernandez-Capetillo O.** 2006. ATM regulates ATR chromatin loading in response to DNA double-strand breaks. J. Exp. Med. **203:**297–303. http://dx.doi.org/10.1084/jem.20051923.
55. **Jazayeri A, Falck J, Lukas C, Bartek J, Smith GC, Lukas J, Jackson SP.** 2006. ATM- and cell cycle-dependent regulation of ATR in response to DNA double-strand breaks. Nat. Cell Biol. **8:**37–45. http://dx.doi.org/10.1038/ncb1337.
56. **Povirk LF.** 1996. DNA damage and mutagenesis by radiomimetic DNA-cleaving agents: bleomycin, neocarzinostatin and other enediynes. Mutat. Res. **355:**71–89. http://dx.doi.org/10.1016/0027-5107(96)00023-1.
57. **Yuan SS, Chang HL, Hou MF, Chan TF, Kao YH, Wu YC, Su JH.** 2002. Neocarzinostatin induces Mre11 phosphorylation and focus formation through an ATM- and NBS1-dependent mechanism. Toxicology **177:**123–130. http://dx.doi.org/10.1016/S0300-483X(02)00220-2.
58. **Lee JH, Kang Y, Khare V, Jin ZY, Kang MY, Yoon Y, Hyun JW, Chung MH, Cho SI, Jun JY, Chang IY, You HJ.** 2010. The p53-inducible gene 3 (PIG3) contributes to early cellular response to DNA damage. Oncogene **29:**1431–1450. http://dx.doi.org/10.1038/onc.2009.438.
59. **Nam EA, Cortez D.** 2011. ATR signalling: more than meeting at the fork. Biochem. J. **436:**527–536. http://dx.doi.org/10.1042/BJ20102162.
60. **Turnell AS, Grand RJ.** 2012. DNA viruses and the cellular DNA-damage response. J. Gen. Virol. **93:**2076–2097. http://dx.doi.org/10.1099/vir.0.044412-0.
61. **Bassermann F, Frescas D, Guardavaccaro D, Busino L, Peschiaroli A, Pagano M.** 2008. The Cdc14B-Cdh1-Plk1 axis controls the G2 DNA-damage-response checkpoint. Cell **134:**256–267. http://dx.doi.org/10.1016/j.cell.2008.05.043.
62. **Bennett LN, Clarke PR.** 2006. Regulation of Claspin degradation by the ubiquitin-proteosome pathway during the cell cycle and in response to ATR-dependent checkpoint activation. FEBS Lett. **580:**4176–4181. http://dx.doi.org/10.1016/j.febslet.2006.06.071.
63. **Mailand N, Bekker-Jensen S, Bartek J, Lukas J.** 2006. Destruction of Claspin by SCFbetaTrCP restrains Chk1 activation and facilitates recovery from genotoxic stress. Mol. Cell **23:**307–318. http://dx.doi.org/10.1016/j.molcel.2006.06.016.
64. **Mamely I, van Vugt MA, Smits VA, Semple JI, Lemmens B, Perrakis A, Medema RH, Freire R.** 2006. Polo-like kinase-1 controls proteasome-dependent degradation of Claspin during checkpoint recovery. Curr. Biol. **16:**1950–1955. http://dx.doi.org/10.1016/j.cub.2006.08.026.
65. **Peschiaroli A, Dorrello NV, Guardavaccaro D, Venere M, Halazonetis T, Sherman NE, Pagano M.** 2006. SCFbetaTrCP-mediated degradation of Claspin regulates recovery from the DNA replication checkpoint response. Mol. Cell **23:**319–329. http://dx.doi.org/10.1016/j.molcel.2006.06.013.
66. **Roos-Mattjus P, Vroman BT, Burtelow MA, Rauen M, Eapen AK, Karnitz LM.** 2002. Genotoxin-induced Rad9-Hus1-Rad1 (9-1-1) chromatin association is an early checkpoint signaling event. J. Biol. Chem. **277:**43809–43812. http://dx.doi.org/10.1074/jbc.M207272200.
67. **Zou L, Cortez D, Elledge SJ.** 2002. Regulation of ATR substrate selection by Rad17-dependent loading of Rad9 complexes onto chromatin. Genes Dev. **16:**198–208. http://dx.doi.org/10.1101/gad.950302.
68. **Ashley AK, Shrivastav M, Nie J, Amerin C, Troksa K, Glanzer JG, Liu S, Opiyo SO, Dimitrova DD, Le P, Sishc B, Bailey SM, Oakley GG, Nickoloff JA.** 10 May 2014. DNA-PK phosphorylation of RPA32 Ser4/Ser8 regulates replication stress checkpoint activation, fork restart, homologous recombination and mitotic catastrophe. DNA Repair (Amst.). http://dx.doi.org/10.1016/j.dnarep.2014.04.008.
69. **Liu S, Opiyo SO, Manthey K, Glanzer JG, Ashley AK, Amerin C, Troksa K, Shrivastav M, Nickoloff JA, Oakley GG.** 2012. Distinct roles for DNA-PK, ATM and ATR in RPA phosphorylation and checkpoint activation in response to replication stress. Nucleic Acids Res. **40:**10780–10794. http://dx.doi.org/10.1093/nar/gks849.
70. **Ikegami S, Taguchi T, Ohashi M, Oguro M, Nagano H, Mano Y.** 1978. Aphidicolin prevents mitotic cell division by interfering with the activity of DNA polymerase-alpha. Nature **275:**458–460. http://dx.doi.org/10.1038/275458a0.
71. **Pedrali-Noy G, Spadari S, Miller-Faures A, Miller AO, Kruppa J, Koch G.** 1980. Synchronization of HeLa cell cultures by inhibition of DNA polymerase alpha with aphidicolin. Nucleic Acids Res. **8:**377–387. http://dx.doi.org/10.1093/nar/8.2.377.
72. **Cotmore SF, Tattersall P.** 1988. The NS-1 polypeptide of minute virus of mice is covalently attached to the 5′ termini of duplex replicative-form DNA and progeny single strands. J. Virol. **62:**851–860.
73. **Cotmore SF, Tattersall P.** 1987. The autonomously replicating parvoviruses of vertebrates. Adv. Virus Res. **33:**91–174. http://dx.doi.org/10.1016/S0065-3527(08)60317-6.
74. **Op De Beeck A, Caillet-Fauquet P.** 1997. The NS1 protein of the autonomous parvovirus minute virus of mice blocks cellular DNA replication: a consequence of lesions to the chromatin? J. Virol. **71:**5323–5329.
75. **Op De Beeck A, Sobczak-Thepot J, Sirma H, Bourgain F, Brechot C, Caillet-Fauquet P.** 2001. NS1- and minute virus of mice-induced cell cycle arrest: involvement of p53 and p21(cip1). J. Virol. **75:**11071–11078. http://dx.doi.org/10.1128/JVI.75.22.11071-11078.2001.
76. **Rogakou EP, Pilch DR, Orr AH, Ivanova VS, Bonner WM.** 1998. DNA double-stranded breaks induce histone H2AX phosphorylation on serine 139. J. Biol. Chem. **273:**5858–5868. http://dx.doi.org/10.1074/jbc.273.10.5858.
77. **Shiotani B, Nguyen HD, Hakansson P, Marechal A, Tse A, Tahara H, Zou L.** 2013. Two distinct modes of ATR activation orchestrated by Rad17 and Nbs1. Cell Reports **3:**1651–1662. http://dx.doi.org/10.1016/j.celrep.2013.04.018.
78. **Vassin VM, Anantha RW, Sokolova E, Kanner S, Borowiec JA.** 2009. Human RPA phosphorylation by ATR stimulates DNA synthesis and pre-

vents ssDNA accumulation during DNA-replication stress. J. Cell Sci. **122:** 4070–4080. http://dx.doi.org/10.1242/jcs.053702.
79. **Charrier JD, Durrant SJ, Golec JM, Kay DP, Knegtel RM, MacCormick S, Mortimore M, O'Donnell ME, Pinder JL, Reaper PM, Rutherford AP, Wang PS, Young SC, Pollard JR.** 2011. Discovery of potent and selective inhibitors of ataxia telangiectasia mutated and Rad3 related (ATR) protein kinase as potential anticancer agents. J. Med. Chem. **54:**2320–2330. http://dx.doi.org/10.1021/jm101488z.
80. **Reaper PM, Griffiths MR, Long JM, Charrier JD, Maccormick S, Charlton PA, Golec JM, Pollard JR.** 2011. Selective killing of ATM- or p53-deficient cancer cells through inhibition of ATR. Nat. Chem. Biol. **7:**428–430. http://dx.doi.org/10.1038/nchembio.573.
81. **Bakkenist CJ, Kastan MB.** 2003. DNA damage activates ATM through intermolecular autophosphorylation and dimer dissociation. Nature **421:** 499–506. http://dx.doi.org/10.1038/nature01368.
82. **Chan DW, Chen BP, Prithivirajsingh S, Kurimasa A, Story MD, Qin J, Chen DJ.** 2002. Autophosphorylation of the DNA-dependent protein kinase catalytic subunit is required for rejoining of DNA double-strand breaks. Genes Dev. **16:**2333–2338. http://dx.doi.org/10.1101/gad.1015202.
83. **Nam EA, Zhao R, Glick GG, Bansbach CE, Friedman DB, Cortez D.** 2011. Thr-1989 phosphorylation is a marker of active ataxia telangiectasia-mutated and Rad3-related (ATR) kinase. J. Biol. Chem. **286:**28707–28714. http://dx.doi.org/10.1074/jbc.M111.248914.
84. **Mohni KN, Smith S, Dee AR, Schumacher AJ, Weller SK.** 2013. Herpes simplex virus type 1 single strand DNA binding protein and helicase/primase complex disable cellular ATR signaling. PLoS Pathog. **9:**e1003652. http://dx.doi.org/10.1371/journal.ppat.1003652.
85. **MacDougall CA, Byun TS, Van C, Yee MC, Cimprich KA.** 2007. The structural determinants of checkpoint activation. Genes Dev. **21:**898–903. http://dx.doi.org/10.1101/gad.1522607.
86. **Berns KI.** 1990. Parvovirus replication. Microbiol. Rev. **54:**316–329.
87. **Luo Y, Lou S, Deng X, Liu Z, Li Y, Kleiboeker S, Qiu J.** 2011. Parvovirus B19 infection of human primary erythroid progenitor cells triggers ATR-Chk1 signaling, which promotes B19 virus replication. J. Virol. **85:**8046–8055. http://dx.doi.org/10.1128/JVI.00831-11.
88. **Wallace NA, Robinson K, Howie HL, Galloway DA.** 2012. HPV 5 and 8 E6 abrogate ATR activity resulting in increased persistence of UVB induced DNA damage. PLoS Pathog. **8:**e1002807. http://dx.doi.org/10.1371/journal.ppat.1002807.
89. **Blackford AN, Patel RN, Forrester NA, Theil K, Groitl P, Stewart GS, Taylor AM, Morgan IM, Dobner T, Grand RJ, Turnell AS.** 2010. Adenovirus 12 E4orf6 inhibits ATR activation by promoting TOPBP1 degradation. Proc. Natl. Acad. Sci. U. S. A. **107:**12251–12256. http://dx.doi.org/10.1073/pnas.0914605107.
90. **Carson CT, Orazio NI, Lee DV, Suh J, Bekker-Jensen S, Araujo FD, Lakdawala SS, Lilley CE, Bartek J, Lukas J, Weitzman MD.** 2009. Mislocalization of the MRN complex prevents ATR signaling during adenovirus infection. EMBO J. **28:**652–662. http://dx.doi.org/10.1038/emboj.2009.15.
91. **Koganti S, Hui-Yuen J, McAllister S, Gardner B, Grasser F, Palendira U, Tangye SG, Freeman AF, Bhaduri-McIntosh S.** 2014. STAT3 interrupts ATR-Chk1 signaling to allow oncovirus-mediated cell proliferation. Proc. Natl. Acad. Sci. U. S. A. **111:**4946–4951. http://dx.doi.org/10.1073/pnas.1400683111.
92. **Mohni KN, Livingston CM, Cortez D, Weller SK.** 2010. ATR and ATRIP are recruited to herpes simplex virus type 1 replication compartments even though ATR signaling is disabled. J. Virol. **84:**12152–12164. http://dx.doi.org/10.1128/JVI.01643-10.
93. **Weitzman MD, Weitzman JB.** 2014. What's the damage? The impact of pathogens on pathways that maintain host genome integrity. Cell Host Microbe **15:**283–294. http://dx.doi.org/10.1016/j.chom.2014.02.010.
94. **Carson CT, Schwartz RA, Stracker TH, Lilley CE, Lee DV, Weitzman MD.** 2003. The Mre11 complex is required for ATM activation and the G2/M checkpoint. EMBO J. **22:**6610–6620. http://dx.doi.org/10.1093/emboj/cdg630.
95. **Zeman MK, Cimprich KA.** 2014. Causes and consequences of replication stress. Nat. Cell Biol. **16:**2–9. http://dx.doi.org/10.1038/ncb2897.
96. **Mohni KN, Dee AR, Smith S, Schumacher AJ, Weller SK.** 2013. Efficient herpes simplex virus 1 replication requires cellular ATR pathway proteins. J. Virol. **87:**531–542. http://dx.doi.org/10.1128/JVI.02504-12.